AIMS Environmental Science

AIMS Environmental Science, 11(5): 831–846.
DOI: 10.3934/environsci.2024041
Received: 21 June 2024
Revised: 02 September 2024
Accepted: 18 September 2024
Published: 24 September 2024

https://www.aimspress.com/journal/environmental

Research article

Exploring the electrical properties of pressboard and kraft paper insulation in power transformers: A dielectric spectroscopy and principal component analysis approach

Souhaib Cherrak[1], Tahar Seghier[1], Ali Benghia[2], Felipe Araya Machuca[3], Augustin Mpanda Mabwe[3] and Souraya Goumri-Said[4,*]

[1] Laboratoire d'étude et de développement des Matériaux Semiconducteurs et diélectriques (LeDMaSD), Algeria
[2] Laboratoire de Physique des Matériaux, University of Amar Telidji, Laghouat, BP 37G, Laghouat 03000, Algeria
[3] Laboratoire SYMADE, Institut Polytechnique UniLaSalle Amiens, 14 Quai de la Somme, 80082 Amiens, France
[4] Department of Physics, College of Science and General studies, Alfaisal University, P.O. Box 5092, Riyadh 11533, Saudi Arabia

* **Correspondence:** Email: sosaid@alfaisal.edu; Tel: +9660111258984.

Abstract: We explored the aging effects on insulating materials used in power transformers through dielectric spectroscopy. Frequency domain spectroscopy (FDS) was conducted for both aged and new Kraft paper and pressboard samples to determine their dielectric properties across a temperature range of 40–100 °C for pressboard and 40–70 °C for Kraft paper. Principal component analysis (PCA) was employed to classify the data, identify key factors contributing to variance, and elucidate the relationships between different parameters. The analysis revealed positive correlations between conductivity and frequency, as well as between permittivity and tan delta, with distinct differences in behavior observed between aged and new samples at lower frequencies. Additionally, the impact of temperature was evident, with increased temperature leading to an upward shift in dielectric behavior. At lower temperatures, aging had a reduced effect on the materials' properties. These findings provide significant insights into the dielectric behavior and aging mechanisms of insulation materials in power transformers.

Keywords: dielectric spectroscopy; frequency domain spectroscopy; aging; principal component

analysis (PCA); paper insulation; power transformers

1. Introduction

Power transformers are critical components within the electrical power grid and are responsible for controlling voltage levels across the entire system. The insulation system of these transformers, primarily comprised of a paper-oil combination, plays a crucial role in maintaining the electrical integrity of the transformer. The condition of this solid insulation directly influences the transformer's lifespan [1–3].

Degradation of the insulation system, commonly occurring due to thermal and mechanical stresses associated with suboptimal operating conditions, accelerates the aging of the paper insulation and increases its susceptibility to both mechanical and electrical failures. This degradation also impacts the oil insulation, where byproducts such as moisture and acids can increase the likelihood of undesirable phenomena, such as partial discharge in both types of insulation, leading to potential electrical failure. Furthermore, paper insulation not only serves as an electrical insulator for the winding conductors but also provides thermal shielding and mitigates mechanical stresses applied to the windings. Consequently, failure in this insulation system can result in significant mechanical failures [1,4].

Pressboard and kraft paper are two widely used materials in the insulation system of power transformers and are the subjects of our study. Pressboard is a composite material made from cellulose fibers that are pressed together to form a dense, strong material with excellent electrical insulation properties. Kraft paper, on the other hand, is a type of paper made from wood pulp and processed with chemicals to enhance its strength and durability [1–4].

To understand the phenomenon of insulation aging and the effect of temperature on insulation parameters, we subjected two samples of both pressboard and kraft paper to accelerated aging in the laboratory. Using frequency domain spectroscopy—a non-destructive measurement method commonly employed in this field—we compiled a database of the electrical properties of both samples. This data spans various temperatures, ranging from 40–100 °C for pressboard and 40–70 °C for Kraft paper.

Presenting and discussing this extensive data posed challenges. Principal component analysis (PCA) was employed to address these challenges. Thanks to its capabilities in dimensionality reduction, noise filtering, data visualization, and feature extraction, PCA enabled us to use different associated plots to cluster our data, visually distinguish the aged samples from the new ones, and explore relationships between parameters. This approach also facilitated the identification of important frequency breakpoints, leading to a more profound understanding of the behavior of the insulation system [5–7].

2. Background on frequency domain spectroscopy

Frequency domain spectroscopy (FDS) is a measurement technique employed to examine the polarization behavior of insulation systems. When dealing with complex mixtures of insulation materials, FDS operates under the assumption that it can detect only overall changes in the insulation than pinpointing localized defects [6]. This technique involves applying a sinusoidal voltage to the test object and measuring both the magnitude and phase of the resulting current. This enables the assessment of parameters such as the dielectric dissipation factor (tanδ) and the complex capacitance/permittivity across a range of frequencies [7,8]. In the context of power transformers, measurements are conducted within a frequency band spanning from 0.01 Hz to 1 kHz to investigate

polarization mechanisms. In our specific case, we conducted these measurements using the IDA200 instrument.

We can describe the dielectric polarization *P* induced within the insulation in relation to the applied electric field *E*, considering that the insulation is humongous and isotropic, with the following expression [9]:

$$P(t) = \varepsilon_0 \chi E(t) \tag{1}$$

where χ is the susceptibility and is related to the relative permittivity ε_r by:

$$\chi = \varepsilon_r - 1 \tag{2}$$

The electric displacement field *D*, in relation to the induced dielectric polarization *P*, is defined as:

$$\begin{aligned} D(t) &= \varepsilon_0 E(t) + P(t) \\ &= \varepsilon_0 E(t) + \varepsilon_0 \chi E(t) \\ &= \varepsilon_0 (1 + \chi) E(t) \\ &= \varepsilon_0 \varepsilon_r E(t) \end{aligned} \tag{3}$$

The total current density *J(t)* inside a dielectric material due to an external electric field according to Maxwell's equations can be given as:

$$\begin{aligned} J(t) &= \sigma E(t) + \frac{\partial D(t)}{\partial t} J(t) \\ &= \sigma E(t) + \varepsilon_0 \frac{\partial E(t)}{\partial t} + \frac{\partial P}{\partial t} \end{aligned} \tag{4}$$

where σ is the DC conductivity of the dielectric material.

By employing either the Fourier or Laplace transformation, and under the assumptions of dielectric linearity and isotropy, with the application of a purely sinusoidal electric field, we can efficiently achieve an analytical transition from the time domain to the frequency domain:

$$\begin{aligned} J(t) &= \sigma E(\omega) + j\omega D(\omega) \\ &= \sigma E(\omega) + j\omega \varepsilon_0 \varepsilon_r E(\omega) \\ &= j\omega \varepsilon_0 \left(\varepsilon_r + \frac{\sigma}{j\omega \varepsilon_0} \right) E(\omega) \\ &= j\omega \varepsilon_0 \bar{\varepsilon}(\omega) E(\omega) \end{aligned} \tag{5}$$

where $\bar{\varepsilon}(\omega)$ is the complex permittivity: $\bar{\varepsilon}(\omega) = \varepsilon'(\omega) - j\varepsilon''(\omega)$.

An expression for the current density can also be written using the complex susceptibility as:

$$\begin{aligned} J(\omega) &= j\omega \varepsilon_0 \left(\varepsilon_r + \frac{\sigma}{j\omega \varepsilon_0} \right) E(\omega) \\ &= j\omega \varepsilon_0 \left(1 + \bar{\chi} - j \frac{\sigma}{\omega \varepsilon_0} \right) E(\omega) \end{aligned} \tag{6}$$

where: $\bar{\chi} = \chi'(\omega) - \chi''(\omega)$.

Thus:

$$J(\omega) = j\omega\varepsilon_0\left(1 + \chi' - j\left(\frac{\sigma}{\omega\varepsilon_0} + \chi''\right)\right)E(\omega)$$

$$= j\omega\varepsilon_0(\varepsilon' - j\varepsilon'')E(\omega) \quad (7)$$

where we can define the components of the complex permittivity as:

$$\varepsilon'(\omega) = Re\big(\bar{\varepsilon}(\omega)\big) = 1 + \chi'(\omega) \quad (8)$$

$$\varepsilon''^{(\omega)} = Im\big(\bar{\varepsilon}(\omega)\big) = \frac{\sigma}{\omega\varepsilon_0} + \chi''(\omega) \quad (9)$$

Note: The expression $\frac{\sigma}{\omega\varepsilon_0} + \chi''(\omega)$ is in phase with the driving field and, therefore, is the term that generates power loss. This term also defines two types of loss: One due to resistive losses caused by conduction and the other due to the inertia of bound and space charges under a changing electric field.

The current I flowing through the dielectric material induced by the external field E can be written as:

$$I(\omega) = j\omega C_0\left(1 + \chi' - j\left(\frac{\sigma}{\omega\varepsilon_0} + \chi''\right)\right)U(\omega) \quad (10)$$

$$I(\omega) = j\omega\bar{C}(\omega)U(\omega) \quad (11)$$

We can define a complex capacitance $\bar{C}(\omega) = C'(\omega) - jC''(\omega)$, where $C'(\omega) = C_0(1 + \chi')$ represents the real capacitance and $C''(\omega) = C_0(\frac{\sigma}{\omega\varepsilon_0} + \chi'')$ is the imaginary capacitance.

The dielectric dissipation factor, commonly referred to as the loss factor, is a metric defined as the ratio between the imaginary part and the real part of impedance. Regarding complex capacitance and permittivity, this relationship can be mathematically represented as follows:

$$tan\delta(\omega) = \frac{\varepsilon''(\omega)}{\varepsilon'(\omega)} = \frac{C''(\omega)}{C'(\omega)} = \frac{\frac{\sigma}{\omega\varepsilon_0} + \chi''}{1 + \chi'} \quad (12)$$

3. Experimental setup and sample preparation

3.1. Experimental setup

IDA 200, the Insulation Diagnostics System used as our measurement equipment as shown in Figure 1, is an apparatus employed for diagnosing high-voltage equipment insulation systems, such as power transformers and cables. It operates by sweeping across frequencies from 0.001 Hz to 1 KHz while applying up to 140 V to the test subject, measuring various dielectric parameters, including the loss factor tanδ, real and imaginary capacitance (C' and C"), and real and imaginary permittivity (ε' and ε") versus frequency [10]. This allows for monitoring the condition of the insulation and understanding its behavior.

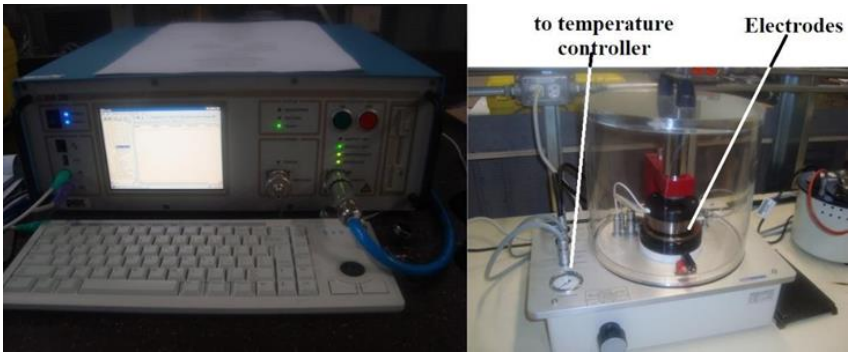

Figure 1. Experimental setup: A diagnostic system and measure cell, respectively.

A custom designed test cell is shown in Figure 2a. The test cell is made of two circular dishes and stainless steel electrodes [11,12]. One of the electrodes has a spring system to provide certain pressure to the sample.

3.2. Sample preparation

Aging manifests within the insulation system of transformers during their extended operational lifespan spanning several decades. Given the impracticality of allowing natural aging in operational environments, the prevailing practice involves replicating this ageing process within controlled laboratory settings through accelerated thermal aging methodologies. This approach affords notable advantages, namely cost-effectiveness, expedited results, and enhanced reliability. It facilitates the generation of specimens endowed with meticulously controlled thermal histories, thereby mitigating the influence of unforeseen variables that may otherwise impact their condition. The paper specimens utilized in our study were prepared following the procedure outlined in [13–15].

To commence the thermal aging process, specimens measuring 81×81 mm were positioned inside a beaker and immersed in 2 liters of oil. Subsequently, metallic catalysts (1 g/l each of zinc, copper, and aluminum) were introduced into a filter paper to replicate the presence of metallic components typically found in transformers. This experimental arrangement was enclosed within a metallic container, sealed using silica gel (Figure 2b) to prevent moisture infiltration, while permitting the simulation of the breathing mechanism observed in free-breathing power transformers. The sealed container was then placed in an oven at 115 °C for 500 hours.

Where: Paper mass= 10 % of the oil mass = 10 % Oil density ×Voil

MPAPER = 0.1 × 0 .85 (Kg /L) × 1.5 L = 141 g

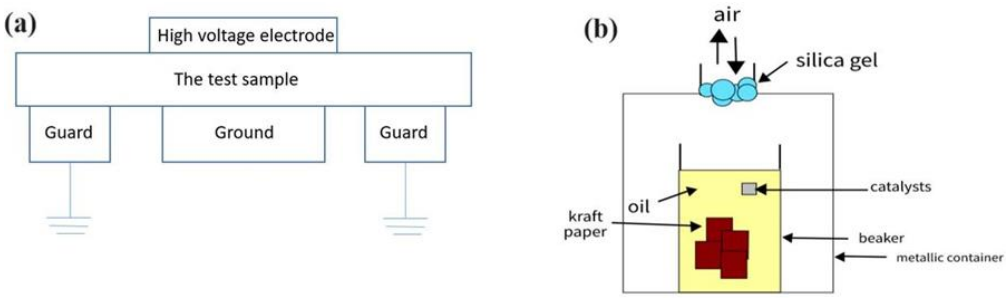

Figure 2. (a) Schematic diagram of the dielectric response measurement system [11]. (b) Schematic representation of aging vessel.

Measurements for various parameters (lose factor, permittivity, and conductivity) conducted using FDS for pressboard at temperatures ranging from 40–100 °C and for kraft paper at temperatures ranging from 40–70 °C.

4. Measurement results

Below, we present graphs for some of the measured parameters using ID200 for both pressboard (from 40–100 °C) and kraft paper (from 40–70 °C). These parameters include the real part of permittivity, dissipation factor, and conductivity.

From Figure 3a,b, the real component of permittivity, denoted as ε', experiences a decline that occurs as frequency increases, eventually stabilizing at higher frequencies for both kraft paper and pressboard, with higher starting values as the temperature continues to increase in an upward shifting trend. It is also noticeable that at high temperatures, non-aged samples have higher starting values compared to aged samples at lower temperatures.

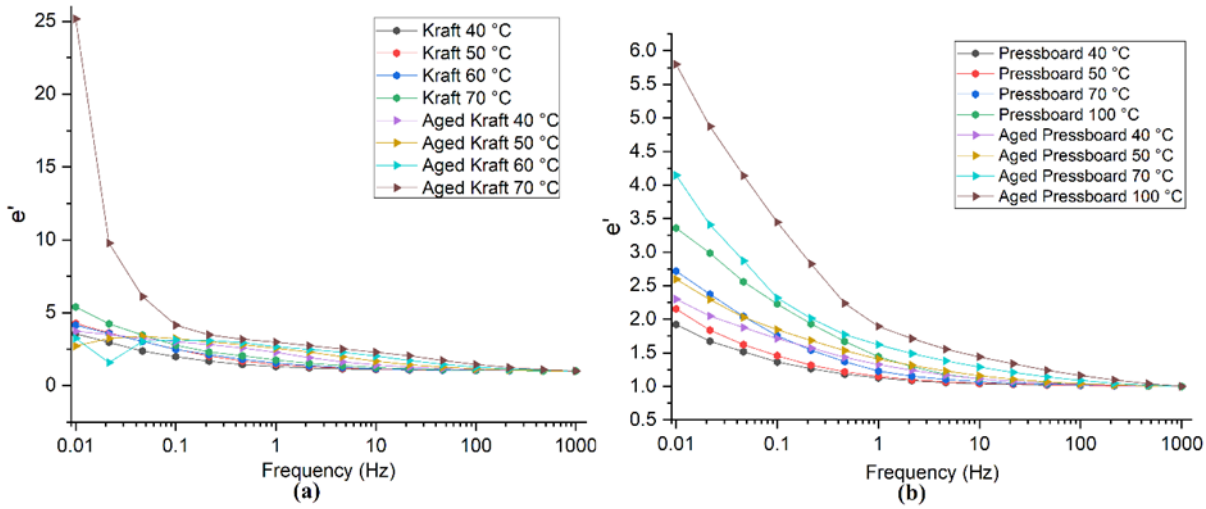

Figure 3. (a) The real part of permittivity for aged and new kraft paper at different temperatures. (b) The real part of permittivity for aged and new Pressboard at different temperatures.

The trend observed in permittivity continues in Figure 4a,b for the dissipation factor. In the case of new samples, the high starting values are due to the increased movement of charge carriers, leading to higher conductivity and losses. This trend extends to aged samples, where it becomes more pronounced due to the depolymerization of the paper's cellulose chains caused by aging. The production of aging byproducts increases the number of charge carriers, further contributing to increased losses.

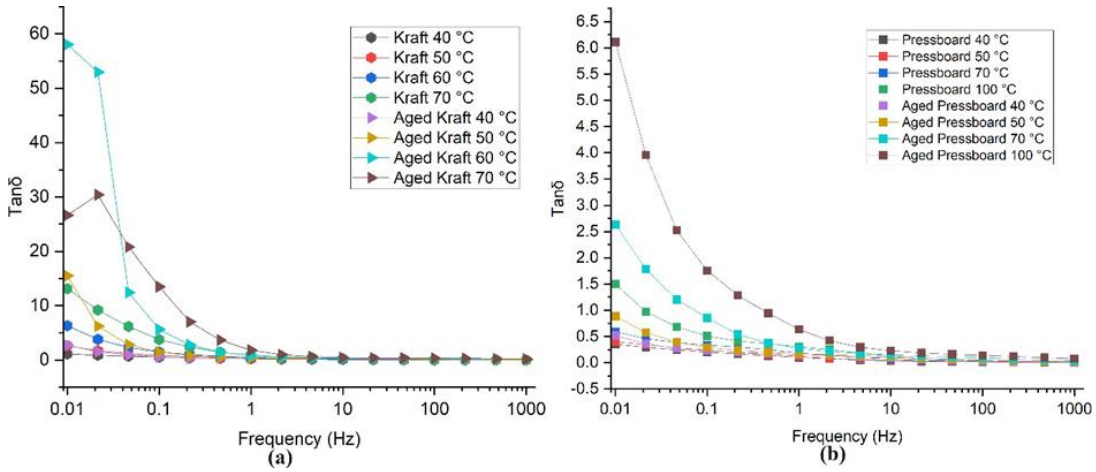

Figure 4. (a) Dissipation Factor for aged and new kraft paper at different temperatures. (b) Dissipation Factor for aged and new Pressboard at different temperatures.

While Figure 5 represents conductivity which increases with the rise in frequency due to the enhanced movement of charge carriers, which is also influenced by the increase in temperature. As stated, aging contributes to an increase in the number of charge carriers, resulting in aged samples of both kraft paper and pressboard having higher values in comparison.

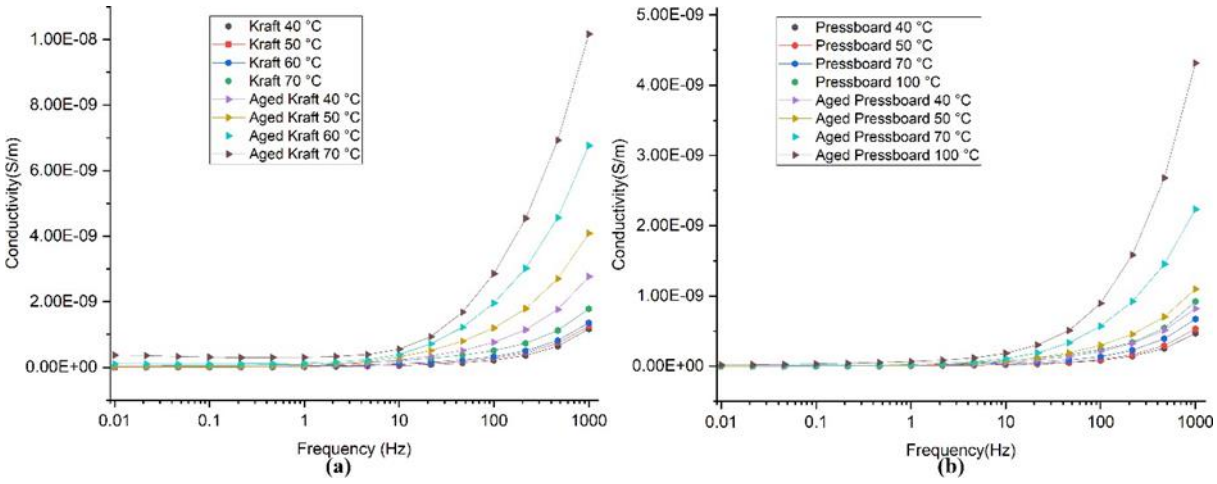

Figure 5. (a) Conductivity of kraft paper at different temperatures. (b) Conductivity of Pressboard at different temperatures.

As it is obvious in the presented Figures, the more data there is, the more difficult it becomes to distinguish representations. While the parameters presented are those commonly used in the literature, they do not provide the full picture because there are relationships between different parameters, and the strength of these relationships changes across different frequency bands. This is without mentioning other unrepresented parameters that could also contribute to a full understanding of the behavior of our insulation system. This is where PCA comes in to solve this problem, as it can represent the entire dataset in one plot while retaining as much as 80% to 90% of the data integrity.

5. Principal component analysis

PCA is a statistical method that reduces the dimensionality of a dataset by identifying patterns and correlations among the variables. The method achieves this by transforming the original dataset into a set of new variables, known as principal components (PC), that capture the maximum amount of variance in the data. The first principal component captures the most significant amount of variance in the data, followed by the second, third, and so on. PCA is particularly useful in analyzing large datasets where the number of variables is high, and the data is noisy or contains redundant information. In the context of dielectric spectroscopy, PCA can be used to identify the dominant factors affecting the dielectric properties of materials, such as pressboard and kraft paper used in power transformers. After pre-processing the data, PCA can be applied to extract the principal components and analyze their contributions to the variance in the data. The resulting principal components can be visualized using biplots, which display the contributions of each variable to the principal components and the relationships among the variables.

PCA was employed in this study as a dimensionality reduction technique to extract the most informative features from the high-dimensional dataset. PCA is a widely used statistical method that aims to transform a set of correlated variables into a smaller set of uncorrelated variables called principal components, while retaining as much of the original variance in the data as possible [16–18]. The first step in performing PCA was to compute the covariance matrix Σ of the centered data matrix X, where each column of X represents a variable, and each row represents an observation. The covariance matrix was calculated as follows:

$$\Sigma = \left(\frac{1}{n-1}\right) \times X^T \times X \tag{13}$$

where n is the number of data points [19,20].

Next, the covariance matrix Σ was decomposed into its eigenvalues and eigenvectors using eigenvalue decomposition:

$$\Sigma = P \times \Lambda \times P^T \tag{14}$$

where P is the matrix of eigenvectors, and Λ is the diagonal matrix of eigenvalues [20].

The principal components were then determined by selecting the eigenvectors of Σ, sorted in descending order of their corresponding eigenvalues. The first principal component is the eigenvector with the largest eigenvalue, the second principal component is the eigenvector with the second-largest eigenvalue, and so on. The data was then projected onto the subspace spanned by the k principal components, where k is the desired number of dimensions to retain. The projection was performed by multiplying the centered data matrix *X* by the matrix of the k principal components P_k:

$$Y = X \times P_k \tag{15}$$

where Y is the projected data matrix in the lower-dimensional space [20].

The number of principal components k to retain was selected based on the proportion of variance explained by each principal component. The goal was to choose the smallest number of principal components that capture a sufficiently large fraction of the total variance in the data, typically 80–90% [20,21]. The use of PCA in this study allowed for the effective reduction of the dimensionality of the dataset while preserving the most relevant information. This preprocessing step was essential for improving the performance and interpretability of the subsequent analyses.

6. Results and discussion

6.1. Preparation of the data

Unlike other studies conducted, this work involves taking two samples (one new and one aged) using an accelerated aging procedure for 500 hours at 115 °C. Measurements were then taken on various temperature points ranging from 40–100 °C for Pressboard and 40–70 °C for Kraft paper on frequencies ranging from 0.01 Hz to 1 kHz. To mitigate potential overlap of data points, we will initially explore the impact of aging on the samples considering the data at only one temperature. Subsequently, we will examine the influence of temperature on both aged and non-aged samples across different temperature [7–11].

6.2. PCA analysis

6.2.1. The effect of aging

Following the execution of PCA on kraft paper and pressboard data each separately, the principal components (PCs) are obtained, each with its individual percentage of the variance in the dataset. Tables 1 and 2 display the cumulative percentage of variance explained by each PC, as well as the individual percentages of variance associated with each PC.

Table 1. Eigenvalues of the correlation matrix of kraft.

PC's	Eigenvalue	Percentage of Variance	Cumulative
1st	6.26354	69.59%	69.59%
2nd	1.55818	17.31%	86.91%
3rd	0.57904	6.43%	93.34%
4th	0.45888	5.10%	98.44%
5th	0.13283	1.48%	99.92%
6th	0.00691	0.08%	99.99%

Table 2. Eigenvalues of the correlation matrix of pressboard.

PC's	Eigenvalue	Percentage of Variance	Cumulative
1st	6.98638	77.63%	77.63%
2nd	1.53442	17.05%	94.68%
3rd	0.31585	3.51%	98.18%
4th	0.07536	0.84%	99.02%
5th	0.06763	0.75%	99.77%
6th	0.01956	0.22%	99.99%

Eigenvalues represent the amount of variance captured by each principal component. The larger the eigenvalue, the more important the corresponding eigenvector is in capturing the variability of the original data. Therefore, the eigenvalues can be used to select the most important principal components

to retain for dimensionality reduction. While percentage of variance and cumulative values are self-explanatory, they can help us determine how many principal components (PCs) we should consider in our study. In the case of the pressboard data, we should consider 3 PCs, which contribute to 97.92% of the variance. For the kraft data, we will also use 3 PCs, since 92.79% is a satisfactory level of variance. This is further confirmed by the scree plot.

PCA typically employs a scree plot to identify the optimal number of PCs, as illustrated in Figure 6a,b. The plot shows the PC number on the x-axis and the corresponding eigenvalues on the y-axis. The point where the eigenvalue sharply rises indicates the number of PCs that are most suitable for the analysis.

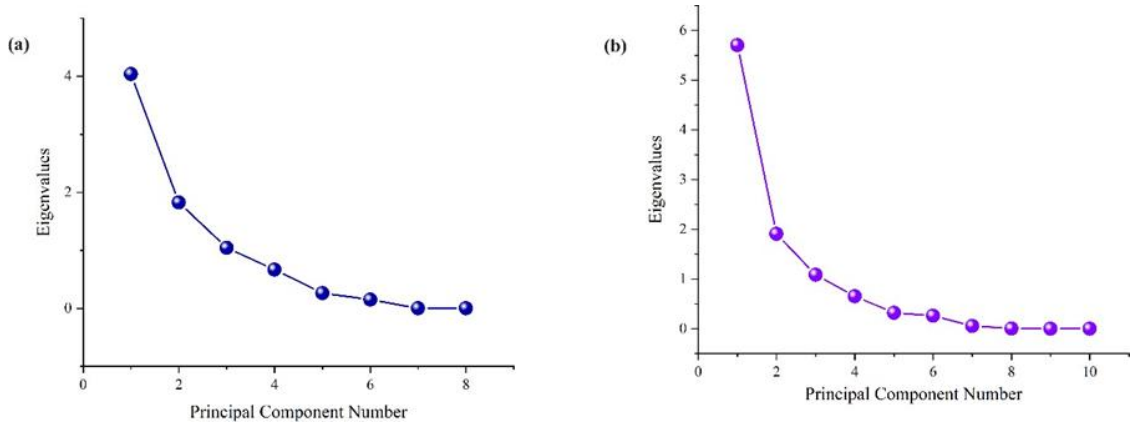

Figure 6. Scree Plot of (a) Pressboard (b) Kraft.

The Scores Plot can provide insights into the underlying structure of the data and can reveal clusters or patterns among the samples. Samples that are close together in the plot are more similar to each other in terms of their multivariate composition [17,18], while samples that are far apart are more dissimilar. The plot can also highlight outliers, which are samples that are distant from the main cluster. In our case, the layout of the data points for both pressboard and kraft paper in Figure 7a,b shows an increase for higher frequencies due to the dominant variance in conductivity, which also increases. However, for lower frequencies, in the case of the aged pressboard sample, the dominant parameter is the capacitance and its real part and for kraft paper is imagery part of capacitance, imagery part of permittivity and dissipation factor.

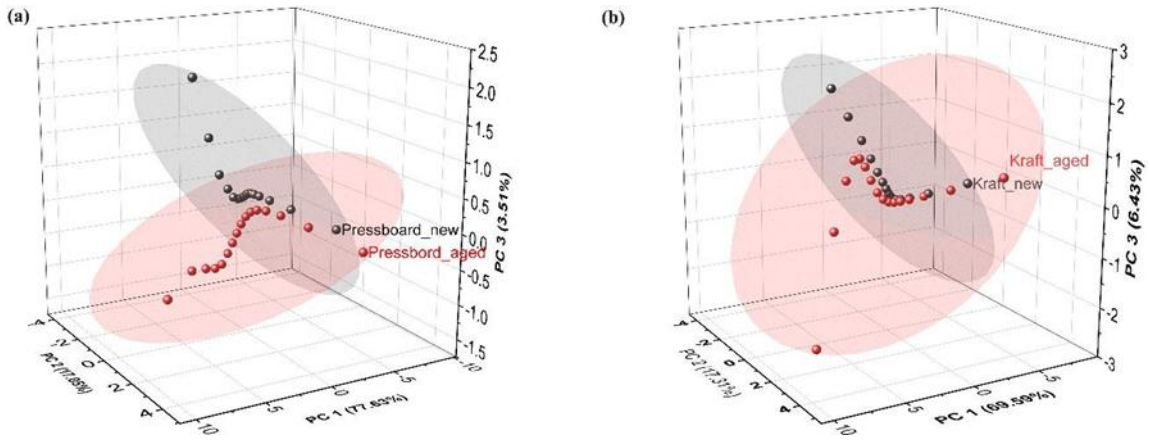

Figure 7. Scores Plot for (a) Pressboard and (b) Kraft paper.

This is further reinforced by biplots in Figure 8a,b. By plotting the observations in the dataset, as well as the variables themselves, on the same graph, biplots allow for the exploration of relationships between the variables, which can help identify any underlying patterns or trends in the data.

We observe in Figure 8a,b a small angle between parameters, such as conductivity and frequency, between imagery parts of both permittivity and capacitance along with the dissipation factor, and between real parts of both permittivity and the capacitance with the capacitance, indicating positive correlations among these parameters. Conversely, there is an angle of about 180 degrees between frequency and dissipation factor, indicating a negative correlation between these parameters.

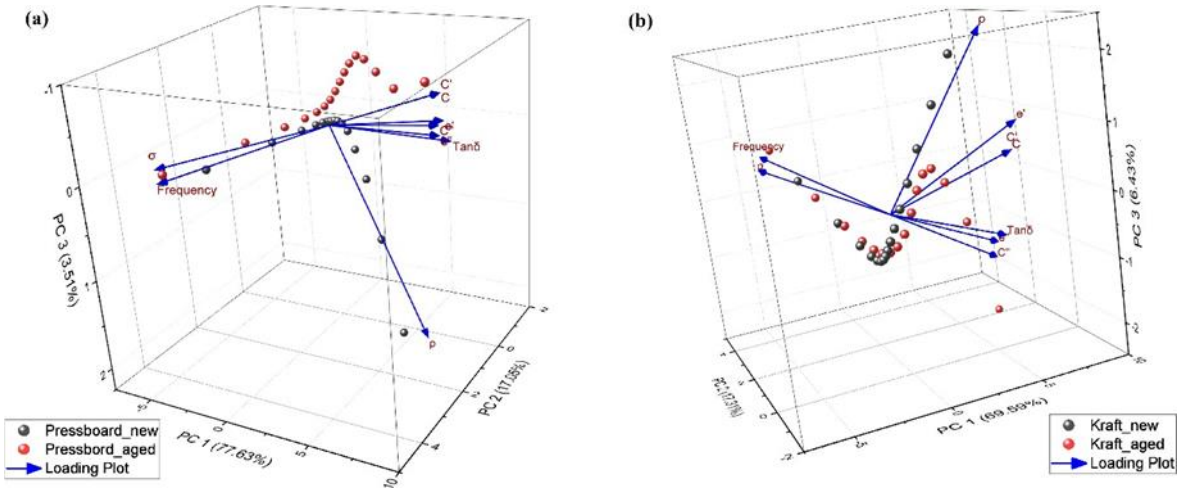

Figure 8. Biplot of the (a) Pressboard (b) the kraft paper.

We can also see in Figure 8a,b divergences between the data points of the aged and new samples at low frequencies, followed by a convergence around 10Hz for pressboard and around 0.1 Hz for kraft paper that is followed by samples behaving the same following along the conductivity vector. This is indicative of the parameter dominating that band from 21.5 Hz to 1 KHz with the aged samples having higher values. We can explain this phenomenon, which arises due to aging induced by product formation (moisture and an increase in acid content), resulting in elevated conductivity and losses. As per Eq 9, it is evident that conductivity contributes to the material's losses, with a more pronounced effect at lower frequencies. This leads to increased losses at lower frequencies. However, as the frequency increases, conductivity loses its significance in determining these losses (around the 21.5 Hz mark) and therefore it becomes the predominant factor influencing this behavior.

6.2.2. Study of the effect of temperature

Usually, when it comes to temperature, its effect on the parameters is described as a vertical shift for most parameters. When it comes to the dissipation factor, that's accompanied by a slight shift to the right as well. we will represent PCA with only 2 components to demonstrate the effect, and we will discuss further when we add the 3rd component.

In the case of kraft paper, three temperatures were chosen: 40 °C, 50 °C, and 70 °C. For pressboard, three temperatures were also selected: 40 °C, 70 °C, and 100 °C. Tables 3 and 4 represent the eigenvalues of the correlation matrix of both papers respectively.

Table 3. Eigenvalues of the correlation matrix of Pressboard at different temperatures.

PC's	Eigenvalue	Percentage of Variance	Cumulative
1st	5.86229	58.62%	58.62%
2nd	1.85396	18.54%	77.16%
3rd	1.05797	10.58%	87.74%
4th	0.7222	7.22%	94.96%
5th	0.27359	2.74%	97.70%
6th	0.22393	2.24%	99.94%

Table 4. Eigenvalues of the correlation matrix of Kraft at different temperatures.

PC's	Eigenvalue	Percentage of Variance	Cumulative
1st	5.70661	57.07%	57.07%
2nd	1.90797	19.08%	76.15%
3rd	1.08693	10.87%	87.02%
4th	0.65306	6.53%	93.55%
5th	0.32127	3.21%	96.76%
6th	0.26223	2.62%	99.38%

Figures 9a and 10a provide valuable insights into the temperature-dependent dielectric behavior of pressboard and kraft paper insulation materials, respectively. In both cases, we observe an overall shift upward and to the right, which becomes more pronounced as the temperature increases along the vector. This observation aligns with the existing literature on the subject.

Moving on to Figure 9b for pressboard samples, we can discern that both aged and new samples exhibit similar behavior at lower temperatures, with resistivity being the dominant factor influencing the dielectric properties. However, as the temperature rises, a noticeable shift occurs. For the aged sample, the real part of capacitance and permittivity emerges as the dominant factor, and this trend further evolves at 100 °C, where the dissipation factor, as well as the imaginary part of capacitance and permittivity, become significant contributors. In contrast, the new pressboard sample exhibits behavior similar to the aged samples at 100 °C, akin to their behavior around 80 °C, but with significantly lower loss values. This distinction highlights the impact of aging on the dielectric response of pressboard insulation at elevated temperatures. The observations made for Figure 9a regarding pressboard samples can be extended to Figure 10a, which depicts the behavior of kraft paper insulation samples. The overall trends and shifts in the dominant factors influencing the dielectric properties are consistent between the two insulation materials, suggesting that the underlying mechanisms governing their temperature-dependent dielectric behavior are similar. These temperature-dependent shifts in dielectric properties, particularly the increase in dielectric losses and the emergence of different dominant factors, can have profound implications for the performance and service life of the insulation systems. As the temperature rises, the aging processes and associated degradation mechanisms accelerate, leading to significant changes in the dielectric response. Understanding these temperature-dependent behaviors is crucial for effective condition monitoring, maintenance strategies, and operational planning in power systems. The insights gained from these observations can inform the development of predictive models, optimized operational parameters, and targeted mitigation

strategies to ensure the reliable and efficient operation of electrical equipment employing pressboard and kraft paper insulation materials.

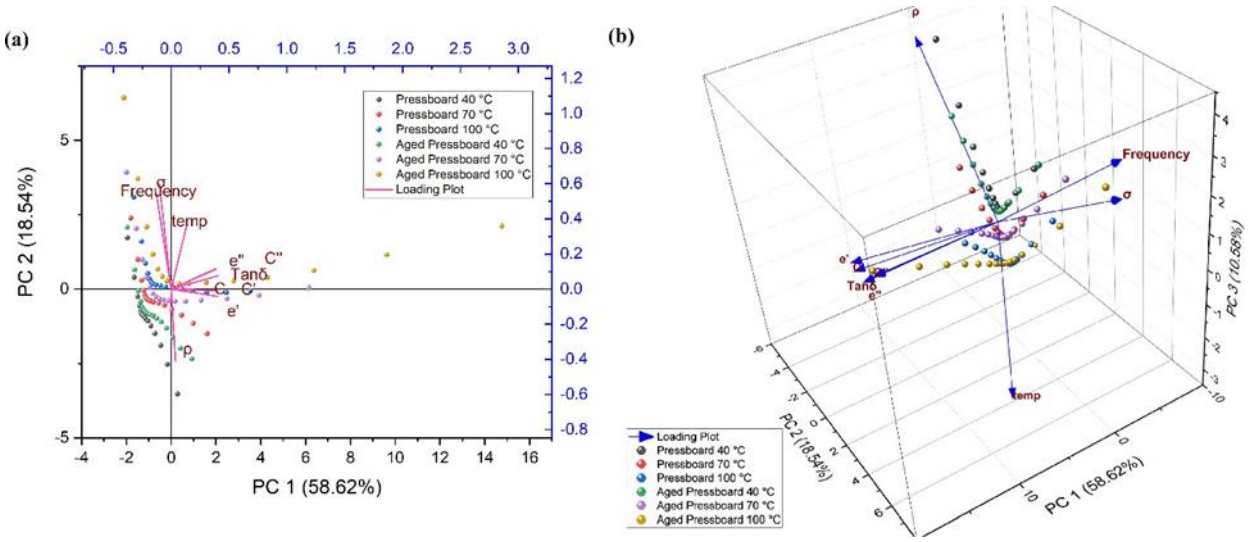

Figure 9. (a) Biplot for Pressboard with 2PC's for different temperature. (b) Biplot for Pressboard with 3PC's for different temperatures.

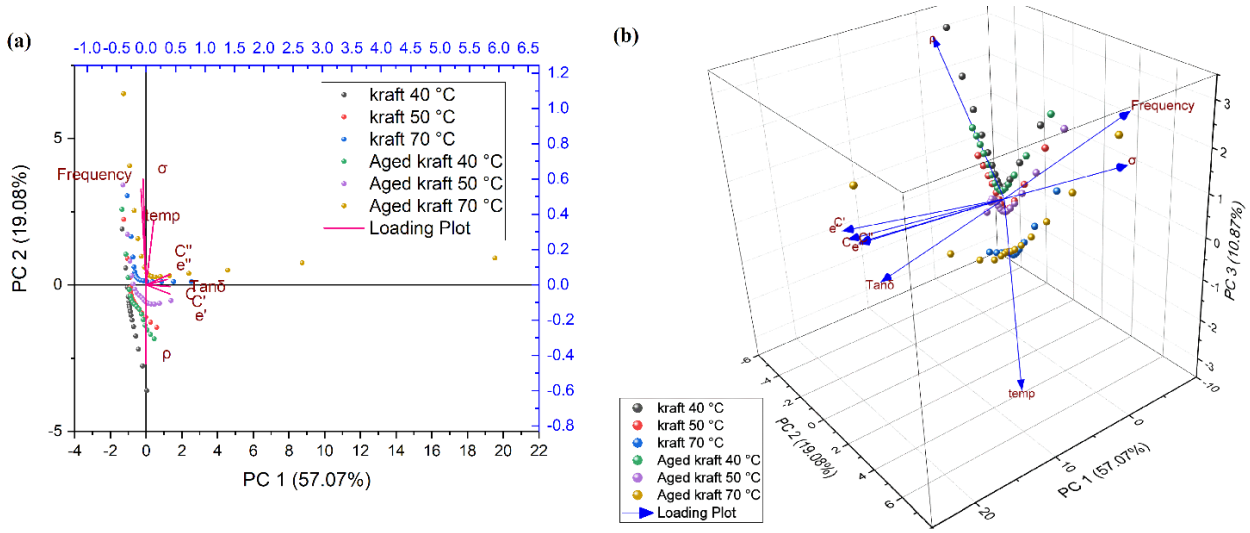

Figure 10. (a) Biplot for kraft paper with 2PC's for different temperature, and (b) Biplot for kraft paper with 3PC's for different temperature.

In Figure 10b, we observe a similar pattern as in Figure 9b, but with a more pronounced shift in the case of kraft paper, even at lower temperatures, compared to pressboard. This phenomenon can be attributed to the following explanation: As the temperature increases from lower values, the heightened thermal energy of the molecules introduces disorder within the insulation material. This disorder leads to a decrease in permittivity and an increase in dielectric losses due to the rise in conductivity. In the case of aged samples, this effect is further exacerbated by the generation of moisture and increasing acid content, resulting in elevated conductivity values even at lower temperatures compared to newer samples, and particularly at higher temperatures. The increase in conductivity observed in aged

samples at elevated temperatures arises from the interplay of two factors: An increase in the density of hopping charge carriers and enhanced mobility among charge carriers within the insulation material [13]. The presence of moisture and acidic byproducts facilitates the formation of charge carriers, while the thermal energy imparted at higher temperatures promotes their mobility, leading to a significant rise in conductivity. This phenomenon is more pronounced in kraft paper compared to pressboard due to the inherent differences in their composition and structure. Kraft paper, being a cellulosic material, is more susceptible to the degradation effects caused by moisture and acidic byproducts, resulting in a more drastic shift in its dielectric properties at lower temperatures. The observed shift in dielectric properties, particularly the increase in conductivity and dielectric losses, can have profound implications for the insulation performance and service life of electrical equipment. These changes may lead to accelerated aging, potential insulation failures, and reduced operational efficiency. Therefore, understanding and monitoring these temperature-dependent dielectric behaviors is crucial for effective condition assessment and maintenance strategies in power systems.

7. Conclusions

We employed FDS to extract crucial parameters such as conductivity, resistivity, dissipation factor, and permittivity, providing valuable insights into the effects of aging processes and temperature on insulation materials. PCA was employed to identify the dominant sources of variance in the data, enabling a useful visualization of the relationships between different parameters. The biplots generated through PCA facilitated the identification of underlying patterns, trends, and correlations within the dataset, leading to the following key observations:

1) Conductivity emerges as the dominant source of variance, exhibiting an increasing trend with frequency. However, for aged samples at lower frequencies, the dissipation factor (tan delta) and the permittivity (especially the imaginary part) become the dominant contributors to the variance an indication of higher losses in the aged sample.
2) In the case of new samples, higher variances are observed in resistivity and resistance parameters, which are indicative of the low losses.
3) Small angles between conductivity and frequency, as well as permittivity and tan delta, indicate positive correlations among these parameters.
4) A large angle of approximately 180 degrees between frequency and dissipation factor suggests a negative correlation between these two variables.
5) To effectively distinguish the condition of the insulation system, it is recommended to focus on parameters such as dissipation factor and permittivity around the frequency band of 21.5 Hz and lower, as conductivity dominates the behavior at higher frequencies, leading to similar responses in both aged and new samples.

It is worth noting that PCA is inherently a linear technique, implying that nonlinear trends caused by nonlinear phenomena in dielectrics, such as the increase in loss and capacitance due to partial discharges, and the nonlinear decrease resulting from the Garton effect and water treeing, may not be fully captured in the results. In such cases, alternative approaches like t-Distributed Stochastic Neighbor Embedding (t-SNE) or non-linear PCA may prove to be more suitable options for capturing these nonlinear effects. This conclusion summarizes the key findings obtained from the FDS and PCA analysis, highlighting the dominant sources of variance, correlations between parameters, and the frequency ranges of interest for distinguishing the condition of insulation systems. Additionally, it acknowledges the potential limitations of PCA in capturing nonlinear phenomena and suggests alternative techniques for future consideration.

Use of AI tools declaration

The authors declare they have not used Artificial Intelligence (AI) tools in the creation of this article.

Acknowledgments

S. Goumri-Said thanks the office of research at Alfaisal University in Saudi Arabia for funding this research work through internal project number 24407.

Conflict of interest

The authors declare that the research was conducted in the absence of any commercial or financial relationships that could be construed as a potential conflict of interest. All Authors contributed equally to this research. All authors have read and approved the final version of the manuscript for publication.

References

1. Yuan Z, Wang Q, Ren Z, et al. (2023) Investigating aging characteristics of oil-immersed power transformers insulation in electrical-thermal-mechanical combined conditions. *Polymers* 15: 4239. https://doi.org/10.3390/polym15214239
2. Liu R, Zhang Z, Nie H, et al. (2020) Effect of mineral oil and vegetable oil on thermal ageing characteristics of insulating paper. *Insul Mater* 53: 65–69
3. Kunakorn A, Pramualsingha S, Yutthagowith P, et al. (2023) Accurate assessment of moisture content and degree of polymerization in power transformers via dielectric response sensing. *Sensors* 23: 8236. https://doi.org/10.3390/s23198236
4. Qiang Fu, Zhang J, Wang M, et al. (2016) Correlation analysis between crystalline behavior and aging degradation of insulating paper, 2016 IEEE International Conference on Dielectrics (ICD), 617–620. https://doi.org/10.1109/icd.2016.7547531
5. Liu F, Cheng L, Gao J, et al. (2019) Characterization of insulation materials used in power transformers using dielectric spectroscopy and principal component analysis. *J Electr Eng Technol* 14: 1651–1659. https://doi.org/10.1007/s42835-019-00027-5
6. Arora R, Rana P (2019) Dielectric spectroscopy: a comprehensive review. *J Mater Sci* 54: 1287–11333. https://doi.org/10.1007/s10853-019-03755-1
7. Baruah N, Sangineni R, Chakraborty M, et al. (2020) Data-driven analysis of aged insulating oils by UV-Vis spectroscopy and principal component analysis (PCA), 2020 IEEE Conference on Electrical Insulation and Dielectric Phenomena (CEIDP), 451–454. https://doi.org/10.1109/CEIDP49254.2020.9437375
8. Saha TK (2003) Review of modern diagnostic techniques for assessing insulation condition in aged transformers, IEEE Transactions on Dielectrics and Electrical Insulation, 10: 903–917. https://doi.org/10.1109/TDEI.2003.1247730
9. Zaengl WS (2003) Dielectric spectroscopy in time and frequency domain for HV power equipment. I. Theoretical considerations. *IEEE Electr Insul M* 19: 5–19. https://doi.org/10.1109/MEI.2003.1238713
10. Insulation diagnostics spectrometer IDA, Programma Electric AB, Eldarv. 4, SE-187 75 Täby, Sweden.

11. Fofana I, Benabed F (2013) Influence of ageing onto the dielectric response in frequency domain of oil impregnated paper insulation used in power transformers, In 9ème Conférence Nationale sur la Haute Tension, 09–11.
12. JäVerberg N, Edin H, Nordell P, et al. (2010) Dielectric properties of alumina-filled poly (ethylene-co-butylacrylate) nanocomposites, 2010 Annual Report Conference on Electrical Insulation and Dielectic Phenomena, 1–4. https://doi.org/10.1109/CEIDP.2010.5724031
13. Shayegani AA, Borsi H, Gockenbach E, et al. (2005) Application of low frequency dielectric spectroscopy to estimate condition of mineral oil, IEEE International Conference on Dielectric Liquids, 285–288. https://doi.org/10.1109/ICDL.2005.1490082
14. Bouaicha A, Fofana I, Farzaneh M (2008) Application of modern diagnostic techniques to assess the condition of oil and pressboard, 2008 IEEE International Conference on Dielectric Liquids, 1–4. https://doi.org/10.1109/ICDL.2008.4622475
15. Setayeshmehr A, Fofana I, Eichler C, et al. (2008) Dielectric spectroscopic measurements on transformer oil-paper insulation under controlled laboratory conditions, IEEE Transactions on Dielectrics and Electrical Insulation, 15: 1100–1111. https://doi.org/10.1109/tdei.2008.4591233
16. Jackson JE (2005) *A user's guide to principal components*, John Wiley & Sons.
17. Jolliffe IT, Cadima J (2016) Principal component analysis: A review and recent developments. *Philos T Roy Soc A* 374: 20150202. https://doi.org/10.1098/rsta.2015.0202
18. Abdi H, Williams LJ (2010) Principal component analysis. *Wires Comput Stat* 2: 433–459. https://doi.org/10.1002/wics.101
19. Shlens J (2014) A tutorial on principal component analysis. *arXiv Preprint* 1404: 1100. https://doi.org/10.48550/arxiv.1404.1100
20. Jolliffe IT (2002) *Principal component analysis*, New York: Springer. https://doi.org/10.1007/b98835
21. Hastie T, Tibshirani R, Friedman J (2009) *The elements of statistical learning: Data mining, inference, and prediction*, New York: Springer.